

A Search for a Surviving White Dwarf Companion in SN 1006

W.E. Kerzendorf,^{1,2*} G. Strampelli,³ K. J. Shen,⁴ J. Schwab,^{5,6} R. Pakmor,⁷
T. Do,⁸ J. Buchner,^{9,10} A. Rest³

¹European Southern Observatory, Karl-Schwarzschild-Straße 2, 85748 Garching bei München, Germany

²ESO Fellow

³Space Telescope Science Institute AURA, 3700 San Martin Drive, Baltimore, MD 21218, USA

⁴Department of Astronomy and Theoretical Astrophysics Center, University of California, Berkeley, CA 94720, USA

⁵Department of Astronomy and Astrophysics, University of California, Santa Cruz, CA 95064, USA

⁶Hubble Fellow

⁷Heidelberger Institut für Theoretische Studien, Schloss-Wolfsbrunnengasse 35, D-69118 Heidelberg, Germany

⁸UCLA Galactic Center Group, Physics and Astronomy Department, UCLA, Los Angeles, CA 90095-1547, USA

⁹Millennium Institute of Astrophysics, Vicuna MacKenna 4860, 7820436 Macul, Santiago, Chile

¹⁰Pontificia Universidad Católica de Chile, Instituto de Astrofísica, Vicuna Mackenna 4860, 7820436 Macul, Santiago, Chile

21 September 2017

ABSTRACT

Multiple channels have been proposed to produce Type Ia supernovae, with many scenarios suggesting that the exploding white dwarf accretes from a binary companion pre-explosion. In almost all cases, theory suggests that this companion will survive. However, no such companion has been unambiguously identified in ancient supernova remnants – possibly falsifying the accretion scenario. Existing surveys, however, have only looked for stars as faint as $\approx 0.1L_{\odot}$ and thus might have missed a surviving white dwarf companion. In this work, we present very deep DECam imaging (u, g, r, z) of the Type Ia supernova remnant SN 1006 specifically to search for a potential surviving white dwarf companion. We find no object within the inner third of the SN 1006 remnant that is consistent with a relatively young cooling white dwarf. We find that if there is a companion white dwarf, it must have formed long ago and cooled undisturbed for $> 10^8$ yr to be consistent with the redder objects in our sample. We conclude that our findings are consistent with the complete destruction of the secondary (such as in a merger) or an unexpectedly cool and thus very dim surviving companion white dwarf.

Key words: ISM: supernova remnants – supernovae: individual: SN1006 – Astrophysics: Solar and Stellar Astrophysics

1 INTRODUCTION

Type Ia supernovae (SNe Ia) are explosions lacking hydrogen and producing copious amounts of ^{56}Ni . This behavior is consistent with thermonuclear burning in a massive ($\geq 0.9M_{\odot}$) degenerate white dwarf (WD). There is no known mechanism for these objects to self-ignite and so theories of the origin of the explosion suggest that the WD can be ignited through binary interaction. For this work, we distinguish between two classes of binary interaction. In one, the WD fully merges with its companion prior to the explosion so that no star remains after the SN Ia occurs. In the

other, the companion remains separate from the exploding WD and survives the explosion.

Detection of a surviving companion star post-explosion would serve to distinguish between the two scenarios (e.g. Marietta et al. 2000; Pakmor et al. 2008; Pan et al. 2013; Shappee et al. 2013). Several groups have attempted to unambiguously identify such a donor star to no avail (e.g. Ruiz-Lapuente 2004; González Hernández et al. 2009; Kerzendorf et al. 2009, 2014; Schaefer & Pagnotta 2012). However, these searches have all focused on relatively bright companions $> 0.1L_{\odot}$, so they could have missed a very faint surviving companion (e.g. a WD; see Shen & Schwab 2017).

Several theories suggest the possibility that the surviving companion is another WD. In double degenerate double detonation scenarios, helium from a He or low-mass C/O

* E-mail: wkerzendorf@gmail.com

Filter	n_{obs}	t_{exp}	FWHM	σ_{FWHM}
-	1	s	1''	1''
u	5	400	1.08	0.07
g	5	50	0.97	0.10
r	5	50	0.85	0.04
z	5	100	0.76	0.03

Table 1. Photometry acquired with DECam on the night of 2017 1 30

WD detonates on the surface of the more massive C/O WD, leading to a carbon core detonation (Fink et al. 2007; Shen & Bildsten 2014). When this He is transferred stably, as in AM Canum Venaticorum binaries (Bildsten et al. 2007), or if the He shell detonates quickly enough after the onset of unstable mass transfer, as in double WD mergers (Guillochon et al. 2010; Pakmor et al. 2013), the less massive companion WD may survive the explosion of the more massive WD. In the single degenerate spin-up/spin-down scenario (Justham 2011; Di Stefano et al. 2011), a C/O WD accretes material from a non-degenerate donor. The accreted angular momentum spins the WD up, allowing it to grow above the canonical (non-rotating) critical mass needed for explosion. However, the accretor WD does not explode until it has spun-down, and during this time the donor star can evolve to become a WD.

Deep photometric searches for surviving companions are difficult because most supernova remnants are located very close to the Galactic Plane (mean and standard deviation of Galactic latitude of remnants $b = 0.07 \pm 2.72$ deg; data from Green 2014) and thus heavily affected by extinction. Fortunately, one of the closest (Winkler et al. 2003) and youngest remnants in the Galaxy, SN 1006 lies very far above the plane ($b = 14.6$ deg) and is only very mildly affected by dust ($A_V \approx 0.3$; Schlafly & Finkbeiner 2011). Thus, SN 1006 is the most promising candidate for a deep search for a possible surviving WD. While previous observations of this remnant (Kerzendorf et al. 2012; González Hernández et al. 2012) have not found any surviving companion, they did not probe deep enough to find a possible surviving WD.

In this work, we present the deepest photometric study so far of SN 1006 using Dark Energy Camera (DECam; Diehl & Dark Energy Survey Collaboration 2012; Flaughner et al. 2015) data and compare the resulting photometry with surviving WD models by various authors.

In Section 2, we present the observations as well as our photometric measurement techniques. In Section 3, we present our techniques to compare the photometry with the suggested surviving WD models. Section 4 confronts the different theoretical scenarios with the analysis performed in this work. We conclude this work in Section 5 and give an overview of future possible tests of the scenarios.

2 OBSERVATIONS & DATA REDUCTION

The images were acquired on the night of 2017 Jan 30 with the Dark Energy Camera (DECam; Diehl & Dark Energy Survey Collaboration 2012; Flaughner et al. 2015) instrument mounted on the 4-m Blanco telescope located at the Cerro Tololo Inter-American Observatory (CTIO). Table 2 shows

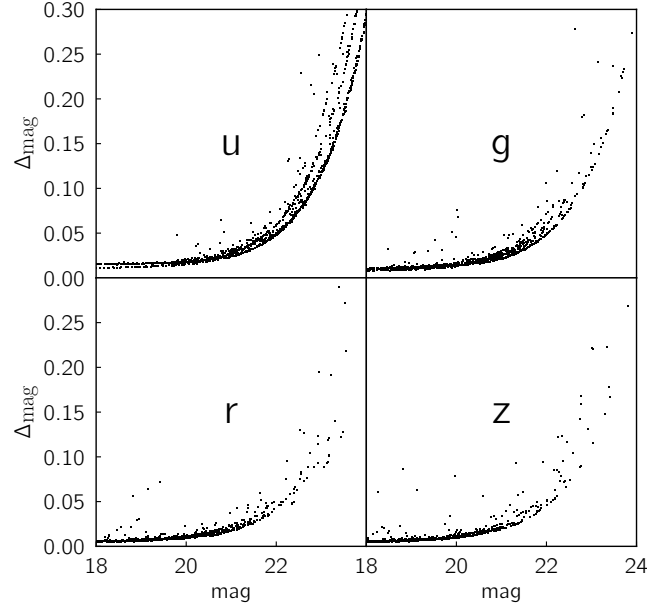


Figure 1. The u , g , r , and z magnitudes with their respective uncertainties of the objects within our search radius of $5'$.

the filter combination, exposure time and seeing in this night using a dither pattern of $\approx 60''$. We used the standard fields sdssj0958_0010 and sdssj1227_0000 in our calibration.

We processed the data using an implementation of the photpipe pipeline modified for DECam images. Photpipe is a robust pipeline used by several time-domain surveys (e.g., SuperMACHO, ESSENCE, Pan-STARRS1; see Rest et al. 2005, 2014), designed to perform single-epoch image processing including image calibration (e.g., bias subtraction, cross-talk corrections, flat-fielding), astrometric calibration, warping and image co-addition, and photometric calibration.

Observations in each filter consists of total of 5 dithered exposures with 62 individual CCD frames per exposure covering the DECam field of view. We process each CCD individually, combining the 5 dither positions per CCD. We use the Two Micron All Sky Survey (Skrutskie et al. 2006) and the IRAF¹ task MSCCMATCH to apply a world coordinate system to the each of the frames using pre-determined distortion terms. This coordinate system then was used to re-project each of the 62 stacks (consisting of the 5 dithered exposures each) to a common coordinate system with the software SWARP (Bertin et al. 2002) using the LANZCOS4 method. We performed DoPhot PSF photometry on each stack resulting in 62 catalogues. This was also done for the standard star fields sdssj0958_0010 and sdssj1227_0000. In a given standard star field image, we have about 120 – 150 stars for rz , 50 – 80 for g , and 20 – 40 for u . We convert the PS1 magnitudes into the DECam natural system AB magnitudes, following the paper by (?). The typical uncertainties

¹ IRAF: the Image Reduction and Analysis Facility is distributed by the National Optical Astronomy Observatory, which is operated by the Association of Universities for Research in Astronomy (AURA) under cooperative agreement with the National Science Foundation (NSF).

in the zeropoint are <0.01 , <0.02 , and <0.03 mags for riz , g , and u , respectively.

For a given filter, we propagate the zeropoints from the standard star fields to the science images, correcting for the airmass, and averaging the zeropoints from the different standard star images. Since we have five standard star images per filter, this decreases the uncertainty by an additional $1/\sqrt{5}$. We apply this mean zeropoint to the SN 1006 image, and create a secondary photometric catalog. Thus the systematic uncertainty in these secondary catalogs is 0.005, 0.01, and 0.015 mags for rz , g , and u respectively.

Finally, the dithering strategy generated stacked images that overlapped and thus the individual catalogues cannot just be appended but need to be merged. In the merging process, we identified stars that were within $1''$ but located on different stacks and co-added those using standard uncertainty propagation rules. This process resulted in the final catalogue for one filter and was repeated for each filter-set.

The final u, g, r, z catalogue was created using a similar merging process with a match distance of 1 arcsecond. The resulting catalogue (limited to our search radius of $5'$ – see Section 3.1) can be seen in Figure 1. The structure seen in the uncertainty is due to the dithering: Stars at the edge of each CCD were observed fewer times than stars near the middle of the CCD. The final catalogue is available at <https://doi.org/10.5281/zenodo.883143>.

3 ANALYSIS

The aim of this experiment is to identify surviving WD companions in SNe Ia explosions.

3.1 Assumptions

For our analysis, we use the remnant’s distance from Winkler et al. (2003) corresponding in a Gaussian prior of 2.07 ± 0.18 kpc (using a conservative value of 2.2 kpc where appropriate).

A conservative estimate of the search area for such a WD (including uncertainties in the center determination) is $5'$ centered around $15^{\text{h}}02^{\text{m}}55.4^{\text{s}} -41^{\circ}56'33''$ (Winkler et al. 2003). This is driven by a maximum escape velocity estimate of a potential WDs companion presented in Shen & Schwab (2017) of $1500 - 2000 \text{ km s}^{-1}$ (corresponding to $2.4 - 3.2'$ at a distance of 2.2 kpc). We use a simple uniform prior that assigns all stars outside of $5'$ of the center ($\approx 1/3$ of the radius; see Figure 3) as having zero probability of being a candidate and all stars within the radius having a uniform probability.

Schlafly & Finkbeiner (2011) give an extinction range estimate of $A_V = 0.26 - 0.30$ assuming an $R_V = 3.1$, which we adopt as a uniform prior for our model. This extinction value is transformed in this work with $A_u/A_V = 1.66$, $A_g/A_V = 1.22$, $A_r/A_V = 0.89$, and $A_z/A_V = 0.48$ to the appropriate filters.

3.2 Theoretical Surviving White Dwarf Models

Figure 2 shows the $u - g/g$ colour magnitude diagram of the candidate stars. For a comparison of the fiducial Shen &

Schwab (2017) models with the data, we approximate surviving WDs with blackbodies (using the data from Table 2) and generate photometry with WSYNPHOT². Figure 2 shows that no viable candidates are near these models.

3.3 White Dwarf Cooling

We extend our search to fainter WD candidates by allowing cooling. The WD cooling curve (Holberg & Bergeron 2006; Tremblay et al. 2011; Bergeron et al. 2011; Kowalski & Saumon 2006) for two masses is shown in Figure 2. Several photometry data points are consistent with old WDs (see Figure 2). The age 10^8 years marked as red crosses, which is approximately when the data and models begin to overlap. In the following sections, we explore the possible parameter space allowed if a surviving white dwarf is in our data set.

3.4 Cooling Models

We approach the exploration of the parameter space of fainter WDs using cooling models. The cooling models in Bergeron et al. (2011)³ with their u, g, r, z photometry are ideal for this task. These models span a mass range of $0.2 - 1.2 M_{\odot}$ with cooling tracks ending at a little more than a few Gyr. We use interpolation (using `SCIPY.INTERPOLATE.CLOUGHTOCHER2DINTERPOLATOR`) to efficiently explore the parameter space and obtain photometry for different ages and masses. Specifically, we use the base-10 logarithm for the interpolation of masses and ages (as the magnitudes behave more linearly in the logarithmic space). Finally, we added a distance modulus and extinction (Schlafly & Finkbeiner 2011) to the interpolated magnitudes resulting in the model $M_{\text{WD}}(\text{mass, age, } d, A_V) \mapsto u, g, r, z$.

3.5 Posterior probability

We explore all possible white dwarf parameters under the assumption that the cooled white dwarf is in our sample. Here we develop the likelihood of any candidate star being a white dwarf of a certain mass, age, d, A_V given the photometric data.

Given a single star and assuming it is a cooling white dwarf with given parameters mass, age, d, A_V , the likelihood to observe its photometric data $D_j = (u_j, g_j, r_j, z_j)$ is:

$$P(D_j | \text{mass, age, } d, A_V) = \mathcal{L}_j \propto \exp\left(-\chi_j^2/2\right) \quad (1)$$

with

$$\chi_j^2 = \left(\frac{u_{j,\text{data}} - u_{\text{model}}}{\sigma_u}\right)^2 + \dots + \left(\frac{z_{j,\text{data}} - z_{\text{model}}}{\sigma_z}\right)^2 \quad (2)$$

We now assume that exactly one of the stars in our sample is the white dwarf. Not knowing which one it is, and assuming each is equally probable a priori, we therefore sum their individual probabilities:

² <https://github.com/wkerzendorf/wsynphot>

³ <http://www.astro.umontreal.ca/~bergeron/CoolingModels/>

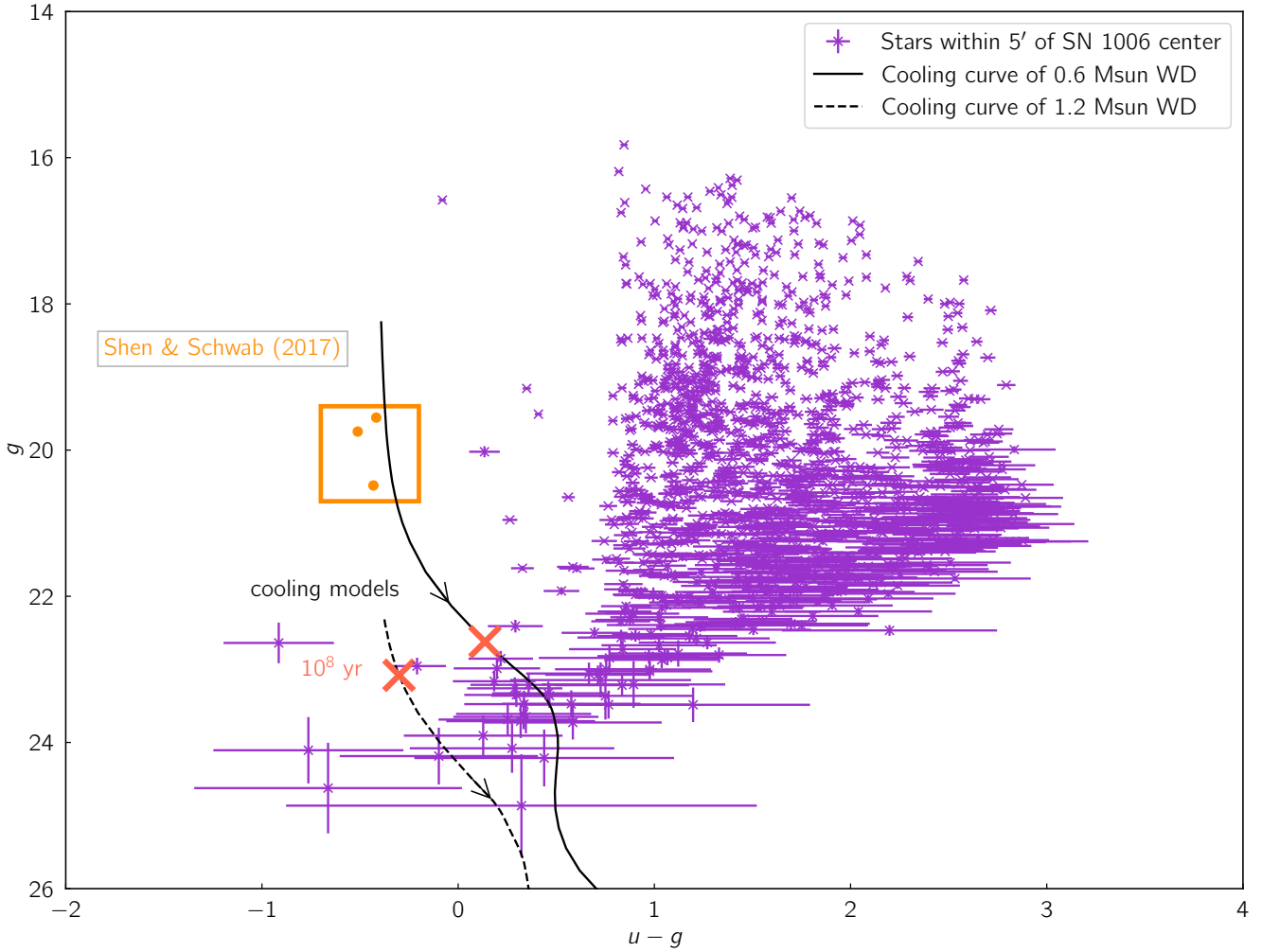


Figure 2. A CMD of all DECAM candidates within $5'$ of the center. In addition, the fiducial blackbody models (assuming an extinction of $A_V = 0.3$; see Table 2) by Shen & Schwab (2017) are in orange circles. We have also added WD cooling curves (solid: $0.6 M_\odot$, dashed: $1.2 M_\odot$; Tremblay et al. 2011) for comparison. The light red crosses on the cooling tracks mark an age of 10^8 years.

Mass M_\odot	Radius km	Temperature 1×10^3 K	u AB mag	g AB mag	r AB mag	z AB mag	$u - g$ AB mag
0.3	15000	45	19.41	19.78	20.17	20.78	-0.37
0.6	9100	50	20.33	20.71	21.12	21.73	-0.38
0.9	6600	150	19.51	19.97	20.44	21.11	-0.46

Table 2. Magnitudes and colors of Shen & Schwab (2017)’s fiducial models at the age of SN 1006 assuming the object to be a blackbody at 2.2 kpc with extinction of $A_V = 0.3$

$$P(D|\text{mass, age, } d, A_V) = \prod_{j=0}^N P(D_j|\text{mass, age, } d, A_V) \quad (3)$$

Following Bayes theorem, to compute parameter probabilities from this likelihood, we need to multiply it with the parameter space priors:

$$P(\text{mass, age, } d, A_V|D) \propto P(D|\text{mass, age, } d, A_V) \times P(\text{mass, age, } d, A_V) \quad (4)$$

We use the priors of Section 3.1. We additionally assume log-uniform prior for the WD age between $10^6 - 10^{10}$ years and a uniform prior for the mass between $0.2M_\odot - 1.2M_\odot$.

3.6 Parameter Space Exploration

The parameter space is sampled using the MULTINEST (Feroz et al. 2009) algorithm and using the implementation available at <https://github.com/kbarbary/nestle>. Figure 4 shows the exploration of the posterior probability including three confidence intervals (68%, 95%, and 99%).

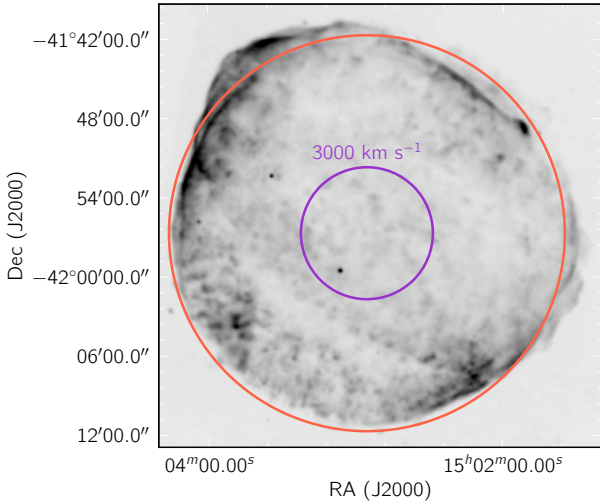


Figure 3. An overview of the SN 1006 remnant in X-rays (0.5 – 0.9 keV) de-noised using the `SCIKIT-IMAGE` (van der Walt et al. 2014) function `SKIMAGE.RESTORATION.DENOISE_TV_CHAMBOLLE` for better visibility. The $\approx 15'$ radius of the remnant around our chosen center is shown as the red circle. We also show our chosen search area which corresponds to the distance moved by an object with a velocity of 3000 km s^{-1} in the plane of the sky.

We have also given an approximate region where the WD with the given parameters would be close or below the detection limit of our data. Figure 5 shows the sample converted from mass and age to temperature and radius (using interpolation). In this figure, we have not marked the areas that are below the detection limit as it is not as straight-forward as with the mass-age parameter space.

4 DISCUSSION

We have placed stringent limits on a surviving companion to SN 1006. We have excluded all young white dwarf models ($\lesssim 10^8 \text{ yr}$) based on a comparison between DECam photometry and theoretical white dwarf models. Previous shallower searches of González Hernández et al. (2012); Kerzendorf et al. (2012) have already ruled out red-giant and main-sequence star companions.

We have compared our photometric data with two methods: Figure 2 shows a traditional visualization of photometric data. Figure 4 and Figure 5 show the posterior probability for any surviving WD existing in the data. The posterior probability for the WD cooling models disallows relatively young WDs with ages of $\lesssim 10^8$ years. At low masses, the cooling curve (solid line in Figure 2) crosses several of our candidate stars at these ages, while at higher masses (dashed line) we have fewer objects. In the probability distribution this makes high masses slightly preferred. The posterior distance probability density distribution is the same as the prior probability.

4.1 Close surviving companion WDs

Double WD binaries have been studied as possible SN Ia progenitor systems in various incarnations for decades (Iben & Tutukov 1984; Webbink 1984). Recent work has raised the possibility that the high temperatures and densities reached during double WD mergers involving a helium or low-mass C/O WD can trigger a helium-powered detonation on the surface of the more massive WD (Guillochon et al. 2010; Raskin et al. 2012; Pakmor et al. 2013). This helium shell detonation can then lead to a carbon core detonation and subsequent SN Ia in a variant of the classic double detonation scenario (Nomoto 1982; Livne 1990; Shen & Bildsten 2014).

The importance of including the necessary isotopes and reaction rates in simulations of helium shell detonations was pointed out by Shen & Moore (2014), who found that such detonations could be triggered in much smaller helium layers than previously realized. This led to the possibility that double detonation SNe Ia could occur early enough in the the double WD merging process that the less massive WD is not completely tidally disrupted when the SN Ia occurs: that is, the less massive companion WD may survive the explosion of the more massive WD.

Double detonations in double WD systems have also been proposed in stably mass transferring AM Canum Venaticorum binaries (Bildsten et al. 2007; Fink et al. 2007; Shen & Bildsten 2009; Fink et al. 2010). For extreme mass ratios, these systems may avoid unstable mass transfer (although see Shen 2015) and lead to accreted helium shells of $\sim 0.01 M_{\odot}$ on the more massive WD. Convection in these shells becomes inefficient and may trigger a helium detonation, which then sets off the core detonation and subsequent SN Ia. The donor WD in these systems will remain undisturbed because it was undergoing stable Roche lobe overflow.

Thus, there are several avenues that may lead to a close-in surviving companion WD following a SN Ia. Shen & Schwab (2017) explored the effect of the ^{56}Ni that is captured from the SN Ia ejecta by nearby surviving WDs. The high temperature and complete ionization of the captured nuclei results in a strongly suppressed ^{56}Ni decay rate, yielding a long-lived luminous outflowing wind. Depending on the mass of the surviving companion and the amount of ^{56}Ni that is captured, the companion may be visible long after the SN Ia occurred.

The orange circles in Figure 2 show the expected g magnitudes and $u - g$ colours of Shen & Schwab (2017)'s fiducial 0.3, 0.6, and $0.9 M_{\odot}$ surviving companion WDs at the present age of SN 1006. It is clear that none of the stars within $5'$ of the remnant's center have the correct magnitude and color to match Shen & Schwab (2017)'s fiducial models. Thus, these models have been ruled out.

However, important caveats remain regarding the appearance of a surviving companion WD. The models of Shen & Schwab (2017) used ad hoc estimates for the amount and thermodynamic conditions of the captured ^{56}Ni mass; in particular, the mass of the captured ^{56}Ni and thus the luminosity should be regarded as an upper limit. A better quantitative estimate of the initial conditions for the outflowing wind requires hydrodynamical simulations that have yet to be undertaken. Furthermore, the models assume

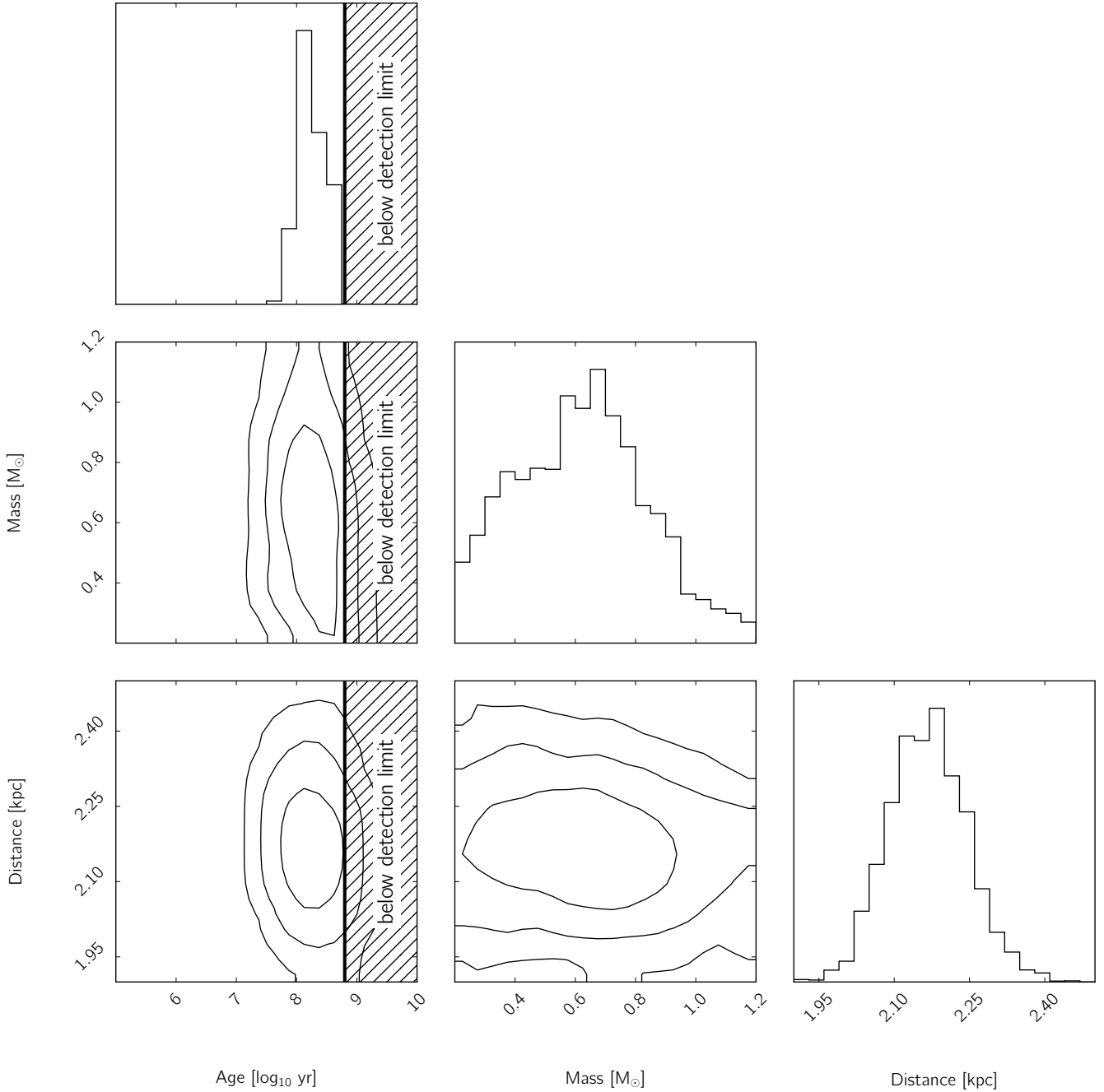


Figure 4. Posterior WD properties given the likelihood and priors in Section 3.5 sampled using NESTLE. We marginalize in these collection of plots over A_V . Note that ages above 10^8 years are preferred.

a constant opacity of $0.2 \text{ cm}^2 \text{ g}^{-1}$ in the ^{56}Ni -rich layer; this is likely a strong underestimate of the true opacity due to iron-group line blanketing. Higher opacities will also significantly alter the luminosity predictions by both increasing the mass outflow rate and changing the colors. An exploration of these effects awaits future simulations; until then, we cannot strongly rule out the presence of a surviving companion WD initially near the explosion site.

4.2 Spin-up/Spin-down model

Justham (2011) and Di Stefano et al. (2011) propose a single-degenerate SN Ia scenario in which the angular momentum of the accreted material spins up the WD, allowing it to grow above the canonical (non-rotating) critical mass needed for explosion ($\approx 1.38 M_{\odot}$). The donor star continues to evolve and in many cases also becomes a WD. Since mass transfer has ceased, the accretor WD spins down and the central density increases, until eventually the explosion is triggered.

The mechanisms of angular momentum loss and redistribution that would operate are uncertain, and thus the

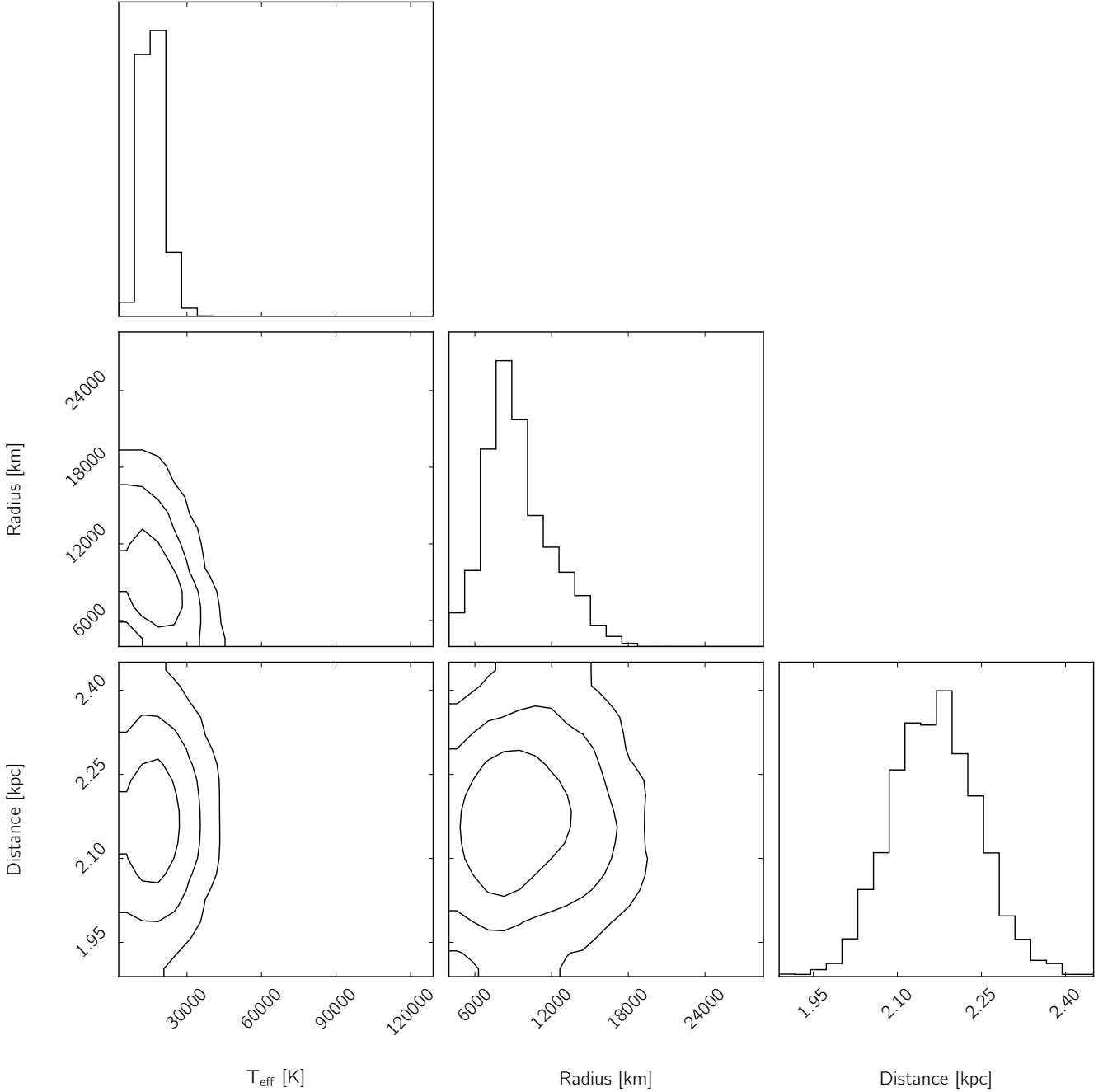


Figure 5. Exploration of the parameter space as given in Figure 4 but using a conversion of the age and mass to radius of temperature by interpolating on the Bergeron et al. (2011) grid. We marginalise in these collection of plots over A_V

delay timescale between the end of mass transfer and the explosion is unknown. Piro (2008) and Neunteufel et al. (2017) find that the WD should be close to solid body rotation during the accretion phase. This implies that one would not form the highly super-Chandrasekhar objects allowed in the presence of differential rotation and suggests the spin-down timescale is not associated with the internal redistribution of angular momentum, but rather the timescale for the loss of angular momentum from the system.

The requirement that the outcome be a normal SNe Ia may itself impose some timescale constraints. For their ro-

tating WD models, Yoon & Langer (2005) suggest that spin-down timescales of $> 10^6$ years imply central densities such that the explosion would violate nucleosynthetic constraints (Iwamoto et al. 1999). Nomoto & Kondo (1991) find that once the accretor WD has crystallized ($\gtrsim 3 \times 10^9$ years), carbon ignition leads instead to accretion-induced collapse.

The data and analysis presented in this paper (see Figure 4) show all possible WDs in SN 1006 are at a minimum a $\approx 10^8$ years old. This provides a significant observational constraint on spin-up/spin-down models as an explanation for “prompt” SNe Ia or for systems that show interaction

with material that must have been produced in the relatively recent past (e.g., nova shells).

5 CONCLUSIONS

We present very deep multi-color (u, g, r, z) photometric data of stars in the center of the SN 1006 remnant in search of surviving WDs. The data show no bright unambiguously identifiable WDs and thus this data is inconsistent with many spin up/down models as well as model presented in Shen & Schwab (2017). This suggests various hypotheses that are consistent with the data. The first hypothesis is that a surviving WD exists but is not as bright as predicted, due to either incorrect assumptions or a limited exploration of parameter space. The majority of red faint objects near the WD cooling curves will likely be foreground stars, but too faint to be detected by Gaia. Unfortunately, many of the other remnants that could be used to test this hypothesis are heavily affected by extinction. This extinction is very detrimental in using the $u - g$ -color to distinguish WDs from unrelated faint fore/back-ground objects. The second hypothesis is that these surviving WD companions do not exist. This hypothesis could be extended (due to the various non-detections of companions in literature) to the claim that generally SNe Ia do not leave any survivors. This would firmly point to the merger and complete disruption of WDs. However, the merger hypothesis has for now no easily falsifiable predictions except for the detection of a companion.

ACKNOWLEDGEMENTS

W. E. Kerzendorf was supported by an ESO Fellowship. Support for this work was provided by NASA through Hubble Fellowship grant # HST-HF2-51382.001-A awarded by the Space Telescope Science Institute, which is operated by the Association of Universities for Research in Astronomy, Inc., for NASA, under contract NAS5-26555. KJS was supported by grants from the NASA Astrophysics Theory Program (NNX15AB16G and NNX17AG28G).

In addition to the software packages mentioned in the paper, we used the following software ASTROPY (Astropy Collaboration et al. 2013), NUMPY (Walt et al. 2011) SCIPY (Jones et al. 2001), PANDAS (McKinney et al. 2010), MATPLOTLIB (Hunter 2007) and APLPY (Robitaille & Bressert 2012) to analyze and visualize the data. This research has made use of NASA's Astrophysics Data System Bibliographic Services as well as the DeepThought literature discovery tool (Kerzendorf 2017).

REFERENCES

- Astropy Collaboration et al., 2013, *A&A*, 558, A33
 Bergeron P., et al., 2011, *ApJ*, 737, 28
 Bertin E., Mellier Y., Radovich M., Missonnier G., Didelon P., Morin B., 2002, in Bohlender D. A., Durand D., Handley T. H., eds, *Astronomical Society of the Pacific Conference Series Vol. 281, Astronomical Data Analysis Software and Systems XI*. p. 228
 Bildsten L., Shen K. J., Weinberg N. N., Nelemans G., 2007, *ApJ*, 662, L95
 Di Stefano R., Voss R., Claeys J. S. W., 2011, *ApJ*, 738, L1
 Diehl T., Dark Energy Survey Collaboration 2012, *Physics Procedia*, 37, 1332
 Feroz F., Hobson M. P., Bridges M., 2009, *MNRAS*, 398, 1601
 Fink M., Hillebrandt W., Röpke F. K., 2007, *A&A*, 476, 1133
 Fink M., Röpke F. K., Hillebrandt W., Seitenzahl I. R., Sim S. A., Kromer M., 2010, *A&A*, 514, A53+
 Flaugher B., et al., 2015, *AJ*, 150, 150
 González Hernández J. I., Ruiz-Lapuente P., Filippenko A. V., Foley R. J., Gal-Yam A., Simon J. D., 2009, *ApJ*, 691, 1
 González Hernández J. I., Ruiz-Lapuente P., Taberner H. M., Montes D., Canal R., Méndez J., Bedin L. R., 2012, *Nature*, 489, 533
 Green D. A., 2014, *Bulletin of the Astronomical Society of India*, 42, 47
 Guillochon J., Dan M., Ramirez-Ruiz E., Rosswog S., 2010, *ApJ*, 709, L64
 Holberg J. B., Bergeron P., 2006, *AJ*, 132, 1221
 Hunter J. D., 2007, *Computing In Science & Engineering*, 9, 90
 Iben Jr. L., Tutukov A. V., 1984, *ApJS*, 54, 335
 Iwamoto K., Brachwitz F., Nomoto K., Kishimoto N., Umeda H., Hix W. R., Thielemann F.-K., 1999, *ApJS*, 125, 439
 Jones E., Oliphant T., Peterson P., et al., 2001, *SciPy: Open source scientific tools for Python*, <http://www.scipy.org/>
 Justham S., 2011, *ApJ*, 730, L34
 Kerzendorf W. E., 2017, preprint, ([arXiv:1705.05840](https://arxiv.org/abs/1705.05840))
 Kerzendorf W. E., Schmidt B. P., Asplund M., Nomoto K., Podsiadlowski P., Frebel A., Fesen R. A., Yong D., 2009, *ApJ*, 701, 1665
 Kerzendorf W. E., Schmidt B. P., Laird J. B., Podsiadlowski P., Bessell M. S., 2012, *ApJ*, 759, 7
 Kerzendorf W. E., Childress M., Scharwächter J., Do T., Schmidt B. P., 2014, *ApJ*, 782, 27
 Kowalski P. M., Saumon D., 2006, *ApJ*, 651, L137
 Livne E., 1990, *ApJ*, 354, L53
 Marietta E., Burrows A., Fryxell B., 2000, *ApJS*, 128, 615
 McKinney W., et al., 2010, in *Proceedings of the 9th Python in Science Conference*. pp 51–56
 Neunteufel P., Yoon S.-C., Langer N., 2017, *A&A*, 602, A55
 Nomoto K., 1982, *ApJ*, 257, 780
 Nomoto K., Kondo Y., 1991, *ApJ*, 367, L19
 Pakmor R., Röpke F. K., Weiss A., Hillebrandt W., 2008, *A&A*, 489, 943
 Pakmor R., Kromer M., Taubenberger S., Springel V., 2013, *ApJ*, 770, L8
 Pan K.-C., Ricker P. M., Taam R. E., 2013, *ApJ*, 773, 49
 Piro A. L., 2008, *ApJ*, 679, 616
 Raskin C., Scannapieco E., Fryer C., Rockefeller G., Timmes F. X., 2012, *ApJ*, 746, 62
 Rest A., et al., 2005, *ApJ*, 634, 1103
 Rest A., et al., 2014, *ApJ*, 795, 44
 Robitaille T., Bressert E., 2012, *APLpy: Astronomical Plotting Library in Python*, *Astrophysics Source Code Library* ([ascl:1208.017](https://ascl.net/1208.017))
 Ruiz-Lapuente P., 2004, *ApJ*, 612, 357
 Schaefer B. E., Pagnotta A., 2012, *Nature*, 481, 164
 Schlafly E. F., Finkbeiner D. P., 2011, *ApJ*, 737, 103
 Shappee B. J., Kochanek C. S., Stanek K. Z., 2013, *ApJ*, 765, 150
 Shen K. J., 2015, *ApJ*, 805, L6
 Shen K. J., Bildsten L., 2009, *ApJ*, 699, 1365
 Shen K. J., Bildsten L., 2014, *ApJ*, 785, 61
 Shen K. J., Moore K., 2014, *ApJ*, 797, 46
 Shen K. J., Schwab J., 2017, *ApJ*, 834, 180
 Skrutskie M. F., et al., 2006, *ApJ*, 131, 1163
 Tremblay P.-E., Ludwig H.-G., Steffen M., Bergeron P., Freytag B., 2011, *A&A*, 531, L19
 Walt S. v. d., Colbert S. C., Varoquaux G., 2011, *Computing in Science & Engineering*, 13, 22

Webbink R. F., 1984, *ApJ*, 277, 355
Winkler P. F., Gupta G., Long K. S., 2003, *ApJ*, 585, 324
Yoon S.-C., Langer N., 2005, *A&A*, 435, 967
van der Walt S., et al., 2014, *PeerJ*, 2, e453

This paper has been typeset from a $\text{\TeX}/\text{\LaTeX}$ file prepared by the author.